Regular Article

IMMUNOBIOLOGY

Classification of human natural killer cells based on migration behavior and cytotoxic response

Bruno Vanherberghen,[1] Per E. Olofsson,[1,2] Elin Forslund,[2,3] Michal Sternberg-Simon,[4] Mohammad Ali Khorshidi,[1] Simon Pacouret,[1] Karolin Guldevall,[1,2] Monika Enqvist,[5] Karl-Johan Malmberg,[5-7] Ramit Mehr,[4] and Björn Önfelt[1-3]

[1]Department of Applied Physics, Albanova University Center, KTH Royal Institute of Technology, Stockholm, Sweden; [2]Advanced Light Microscopy, Science for Life Laboratory, Solna, Sweden; [3]Department of Microbiology, Tumor and Cell Biology, Karolinska Institutet, Stockholm, Sweden; [4]The Mina and Everard Goodman Faculty of Life Sciences, Bar-Ilan University, Ramat-Gan, Israel; [5]Center for Infectious Medicine, Department of Medicine, Karolinska Institutet, Stockholm, Sweden; [6]Department of Immunology, Institute for Cancer Research, Oslo University Hospital, Oslo, Norway; and [7]Faculty of Medicine, Oslo University, Oslo, Norway

---

Key Points

- Activated NK cells display heterogeneity in their cytotoxic responses that justifies grouping them into 5 distinct classes of NK cells.
- A subpopulation of particularly active "serial killer" NK cells deliver their lytic hits faster and release more perforin in each hit.

Despite intense scrutiny of the molecular interactions between natural killer (NK) and target cells, few studies have been devoted to dissection of the basic functional heterogeneity in individual NK cell behavior. Using a microchip-based, time-lapse imaging approach allowing the entire contact history of each NK cell to be recorded, in the present study, we were able to quantify how the cytotoxic response varied between individual NK cells. Strikingly, approximately half of the NK cells did not kill any target cells at all, whereas a minority of NK cells was responsible for a majority of the target cell deaths. These dynamic cytotoxicity data allowed categorization of NK cells into 5 distinct classes. A small but particularly active subclass of NK cells killed several target cells in a consecutive fashion. These "serial killers" delivered their lytic hits faster and induced faster target cell death than other NK cells. Fast, necrotic target cell death was correlated with the amount of perforin released by the NK cells. Our data are consistent with a model in which a small fraction of NK cells drives tumor elimination and inflammation. (*Blood*. 2013;121(8):1326-1334)

Introduction

Natural killer (NK) cells were first reported almost 40 years ago as cells exhibiting spontaneous, nonadaptive cell-mediated cytotoxicity.[1] Today, they are known for their ability to both eliminate infected or transformed cells without prior antigen-dependent activation and to secrete immunomodulatory cytokines regulating adaptive immune responses.[2] Molecularly, the NK response is regulated by activating and inhibitory signals received at the zone of tight intercellular contact, the immune synapse (IS).[3-6] Efforts have focused on understanding the molecular dynamics at the IS and the biophysical mechanisms involved.[7] Although much has been learned, little is known about how the responses of individual NK cells sum up to functional properties at the population level. Many basic questions remain unanswered: Are all NK cells efficient killers? How do NK cells behave in successive contacts? How many target cells can an NK cell kill? Clearly, differences between the responses of individual NK cells could have consequences at the population level.

At a single-cell level, it is known that NK cell killing is tightly regulated because it has to clear several checkpoints before delivery of a targeted cytolytic response.[8,9] Checkpoints include transport of the lytic granules to the microtubule organizing center,

polarization of the organizing center to the IS, and release of granules through holes in the actin mesh directly into the central region of the NK cell IS.[3,10] For the elimination of virus-infected or tumor cells, the main mechanism of NK cell–mediated cytotoxicity is by exocytosis of granules containing granzymes and perforin into the IS.[11,12] Granzymes induce apoptotic death, whereas perforin induces substantially faster death accompanied by formation of large membrane protrusions.[13] Although a fraction of NK cells can deliver a lytic hit in less than 10 minutes, a general overview of NK cell killing dynamics is lacking.[8,14,15] Both single T cells and NK cells have been observed to kill up to 6 target cells sequentially, coinciding with a decrease in both perforin and granzymes.[16-18] No data are available regarding the frequency of such "serial killers" within cell populations. On average, a single IL-2–activated NK cell could kill 4 target cells in 16 hours.[17] However, NK cells could have the potential to kill many more if recycling cytotoxic molecules.[19,20] Eventual depletion of perforin in granules is thought to contribute to "exhaustion" of the NK cells' killing capacity.

Although flow cytometry allows phenotypic classification of NK cells, one of the primary challenges to achieving a detailed

---

characterization of NK cell behavior has been to follow individual cells for extended periods of time (several hours). Here, we have used a microchip-based approach where cells are confined while being imaged,[21] and followed individual NK cells for 12 hours as they make consecutive interactions with target cells. We observed a significant heterogeneity in individual NK cell responses, with some cells unable to kill target cells and others able to kill up to 7 target cells with high fidelity. NK cells induced either fast or slow target cell death, which was correlated with necrotic or apoptotic death, respectively. Interestingly, a minority of the NK cells was responsible for the majority of the killing events. Finally, serial killers killing 5 or more target cells were responsible for a large proportion of the necrotic killing events.

Methods

Cell culture

The adherent human embryonic kidney 293T cell line was cultured in RPMI 1640 medium supplemented with 10% fetal calf serum, 2mM L-glutamine, 1× nonessential amino acids, 1mM sodium pyruvate, 50 U/mL of penicillin-streptomycin, and 50μM β-mercaptoethanol. Human polyclonal NK cells were isolated from healthy donor peripheral blood by negative magnetic bead selection according to the manufacturer's instructions (StemSep, StemCell Technologies). Freshly isolated NK cells were cultured in Iscove modified Dulbecco medium supplemented with 10% human serum, 2mM L-glutamine, 50 U/mL of penicillin-streptomycin, 1mM sodium pyruvate, 1× nonessential amino acids, 50μM β-mercaptoethanol, and 100 U/mL of IL-2 (NK cell medium). NK cell purity was > 95% $CD3^-CD56^+$ (dim) and cells were used between 9 and 16 days after isolation.

Cell labeling

For 1,1′-dioctadecyl-3,3,3′,3′-tetramethylindodicarbocyanine perchlorate (DiD) labeling, 10^6 cells/mL were loaded with 4 μg/mL of DiD in RPMI 1640 medium at 37°C and 5% CO_2 for 15 minutes. For calcein-AM and calcein red-orange (10^6 cells/mL) were loaded with 1μM/mL or 0.4μM/mL, respectively at 37°C and 5% CO_2 for 10 minutes. After staining, cells were washed twice in RPMI 1640 culture medium. Fluorescent probes were purchased from Invitrogen.

Cytotoxicity assay

NK cell cytotoxicity was measured by standard chromium release with 5×10^4 radiolabeled target cells. Spontaneous target cell lysis was < 20%.

CD107a degranulation assay

IL-2–activated NK cells were cocultured with DiD-labeled 293T cells at various effector to target (E:T) ratios. To mimic the chromium-release assays, the number of 293T cells was kept constant (50×10^4/well) and the number of NK cells was titrated down. Cocultures were performed in NK cell medium for 4 hours in the presence of GolgiStop (BD Biosciences) and 1 μg/well of anti-CD107a–FITC. Cells were then stained with anti-CD56–PE to identify NK cells. NK cells were gated on ($CD56^+DiD^-$) and the frequency of $CD107a^+$ NK cells was scored. At least 500 NK events were acquired.

Melittin assay

Calcein-AM–labeled 293T cells were seeded into flat-bottom 96-well plates and left to adhere for 1 hour. Bright-field and calcein fluorescence was acquired with a 20× objective at 3-second intervals for 2-3 minutes with an open pinhole using a LSM 780 inverted confocal microscope (Zeiss). Directly after imaging was started, melittin (Sigma-Aldrich) was added directly to give final concentrations of 4.65, 6.25, or 8.33 μg/mL. Cells exposed to 4.65 and 6.25 μg/mL were confirmed to be viable 24 hours after exposure.

Imaging in microwells

Imaging was performed as described previously.[21] Briefly, 20×10^5 cells/mL of calcein-AM–labeled 293T cells were seeded onto a dry silicon-glass microchip containing 650×650 μm^2 wells and left to adhere to the glass surface for 30 minutes at 37°C and 5% CO_2. Calcein red-orange–labeled polyclonal NK cells were subsequently seeded at 10^5 cells/mL for 5 minutes until 50-100 NK cells were present in each well. Excess cells and media were removed and the chip was submerged in NK cell medium and imaged at a 10× magnification (Plan-Neofluar air objective, numeric aperture 0.30) using an LSM 5 Pascal confocal microscope (Carl Zeiss) equipped with an environmental chamber kept at 37°C and 5% CO_2. The pinhole was opened to capture maximum fluorescence and images were acquired every 2 minutes for approximately 12 hours. The data presented are pooled from 3 experiments.

Image analysis

NK cells were manually tracked using Volocity 5.4.0 software (Improvision) based on their fluorescence and each interaction with a target cell was scored. Conjugates were defined as periods longer than 4 minutes when opposing NK and target cell membranes appeared flat. Adhesion periods were defined when NK cells had a migratory, elongated shape while remaining in physical contact with the target cells. Target cell death was detected by calcein leakage from the target cells and by visual signs of death in the bright-field image (ie, blebbing or swelling).

Analysis of the calcein intensity decay during target cell death

Rate of decay. Calcein fluorescence intensity was quantified as a function of time using ImageJ 1.45 software. Target cell bleaching was significantly different from the decay associated with target cell death. To analyze objectively the rate of calcein leakage during target cell death, the decay profiles were fitted to a sum of 3 exponentials:

$$I = \alpha_1 e^{-t/\tau_1} + \alpha_2 e^{-t/\tau_2} + \alpha_3 e^{-t/\tau_3} + C$$

The 3 lifetimes $\tau_1 - \tau_3$ were fixed to 0.5, 20, and 50 minutes because this combination gave satisfactory fits to most intensity decays. The shortest lifetime was shorter than the frame rate used in the experiment and thus essentially functioned to fit any rapid intensity decrease observed at the beginning of the decay. To compare individual decays with each other, an average lifetime was formed according to:

$$\tau_{mean} = \alpha_1 \tau_1 + \alpha_2 \tau_2 + \alpha_3 \tau_3$$

where α_1-α_3 are the normalized preexponential coefficients so that $\alpha_1 + \alpha_2 + \alpha_3 = 1$. Fast decays were defined based on their mean lifetime being ≤ 10 minutes.

Multiple lytic hits. Several consecutive decreases in calcein fluorescence within a single conjugation period were quantified and characterized by a combination of manual, visual inspection, and automatic analysis (inhouse MATLAB routine). A successive hit was scored if there was a clear arrest in calcein decay for at least 4 minutes between 2 decreases greater than 9% of the maximum fluorescence intensity. The maximum fluorescence was obtained using the mean of the 3 largest intensity values scored for that particular target cell.

Analysis of NK cell size

Individual NK cell area was measured at each time point by expanding an image (45×45 μm^2) around the trajectory coordinate in which the NK cell could be segmented.[22] Abnormal values (eg, due to segmentation of cell clusters) were excluded and the mean values from all valid points in the trajectory were formed.

Computer simulations

A model was designed that simulated a homogeneous population of NK cells (n = 534) cocultured with target cells (n = 2400), allowing NK cells to move in and out of contacts with target cells for 12 hours (see model scheme in supplemental Figure 1, available on the *Blood* Web site;
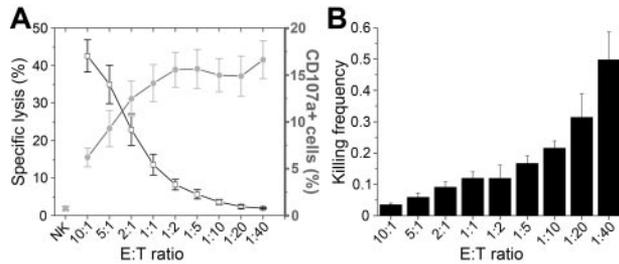
Figure 1. Population-based analysis of NK cell lysis. (A) Percentage of target cell lysis (black open squares and line) and the percentage of CD107a+ NK cells (gray circles and line) over decreasing E:T ratios. Values plotted are means with SE from at least 4 independent experiments. (B) NK cell killing frequency (number of target cells killed per NK cell) calculated from the data in panel A.

see the Supplemental Materials link at the top of the online article). The probability of NK-mediated killing was set to 58% in all NK-target contacts based on the experimental data. The contact duration and the times between contacts were based on the experimental distributions. The number of simultaneous contacts an NK cell could participate in was limited to 2.

Statistical analysis

The Student t test, Mann-Whitney U test, Yates χ^2 test, or Fisher exact test were used to evaluate statistical significance as appropriate.

Results

Population-based lysis and degranulation experiments

The ability of IL-2–activated NK cells to lyse 293T target cells was tested in 2 standard population-based assays: chromium release and CD107a degranulation. The chromium-release assay reflects the amount of target cells lysed and CD107a staining yields information on the percentage of degranulating NK cells (Figure 1A).[23] At high E:T ratios, the number of target cells lysed reached 40%; therefore, despite being surrounded by a large excess of NK cells, most target cells were not killed during the 4-hour assay. As NK cells were titrated down, killing of 293T cells decreased until it was undetectable at E:T ratios below 1:10. The percentage of NK cells in which degranulation was detected was lowest at the highest E:T ratio and increased as NK cells were titrated down, reaching a plateau of approximately 15% for E:T ratios lower than 1:2 (Figure 1A). Therefore, target cell lysis is increased at high E:T ratios, but at the same time it is less likely that all potentially reactive NK cells will encounter target cells and degranulate. Conversely, at higher relative densities of target cells, it is more likely that all NK cells encounter target cells that can trigger degranulation. Consistent with this interpretation, the killing frequency of NK cells, the average number of target cells killed per NK cell, increased with decreasing E:T ratios (Figure 1B). At the lower E:T ratios, the average NK cell killed approximately 0.3-0.5 target cells. Therefore, if only 15% of NK cells were degranulating, each active NK cell must kill several target cells during the incubation. These results indicate that a fraction of the NK cells were capable of killing several target cells, but this type of analysis yields no information about what occurs at the single-cell level.

Microchip-based assay allowing detailed characterization of NK-target cell interactions

To investigate NK cell killing at the single-cell level, small populations of NK cells (40-80) were imaged and tracked as they migrated and interacted with a population of adherent 293T cells (250-300) within microwells.[21] With this approach, individual NK cells could be followed over an extended period of time, allowing the entire contact history of each NK cell to be recorded. In three 12-hour time-lapse experiments, 178 NK cells were followed and the outcome of 384 NK-target conjugates was scored. Conjugation and killing were visible throughout the time-lapse sequences (supplemental Figure 2).

Broadly, the NK-target interaction could be described by 3 different phases: migration, conjugation, and attachment (Figure 2). During migration, NK cells moved freely without physical contact with target cells. When reaching a target cell, the NK cell often rounded up, forming a flattened intercellular contact with the target cell. During this conjugation phase, the NK cells sometimes (58% of all interactions) delivered a lytic hit detected by a sudden decay in the target cell calcein fluorescence in conjunction with morphologic signs of death (ie, cell explosion or membrane blebbing). On dissociation of the NK-target conjugate, the NK cell resumed an elongated shape and often the target cell (73% of the time) remained attached to the NK cell, sometimes being dragged along as the NK cell migrated away.[14] Eventually, the NK cell detached from the target cell and either resumed free migration or conjugated with another target cell. Detachment was sometimes accompanied by the formation of membrane nanotubes connecting the NK and target cell.[14,24] Individual NK cells were sometimes observed to engage in several contacts simultaneously. To characterize NK-target cell interaction dynamics, we defined 4 different times: the conjugation time, the attachment time, the time between initiation of conjugation and delivery of the lytic hit, and the time between the lytic hit and the first visible signs of target cell death (Figure 2).

Conjugation and attachment times for lytic and nonlytic interactions

The mean conjugation time was shorter for lytic compared with nonlytic interactions (65 vs 81 minutes), indicating that the decision to end a stable contact was made faster when killing occurred. However, the spreads of conjugation times were large for both nonlytic and lytic interactions, with the majority of conjugates (60% and 67% of nonlytic and lytic conjugates, respectively) lasting less than 1 hour and a small number of conjugates (7% and 4% of nonlytic and lytic conjugates, respectively) lasting ≥ 3 hours (Figure 3A). Lytic interactions more frequently resulted in an attachment period than nonlytic interactions (80% vs 63%). In the events in which attachment periods were detected, no statistically significant difference was found between the mean attachment length for nonlytic and lytic interactions (128 and 154 minutes, respectively, Figure 3B). However, target cells were displaced further during the attachment phase in lytic compared with nonlytic interactions (83 vs 58 μm), which could reflect a difficulty in breaking strong receptor-ligand interactions when activating signals predominate or loss of substrate adherence when dying. Therefore, these data show that stable NK-target contacts were shorter in lytic interactions and that target cells often spend a significant amount of time attached to NK cells directly after periods of stable conjugation.

Rapid delivery of the lytic hit and subsequent target cell death

All target cells contacted by NK cells were monitored and analyzed for both visible signs of death in the bright-field image and the

Figure 2. NK cell surveillance involves the dynamic phases migration, conjugation, lytic hit, and attachment. (A) Schematic representation of the process of NK-target cell interaction. Top: NK cell (red) migrating to form a conjugate with a target cell (green) leading to NK-mediated killing of the target cell as detected by decreased intracellular calcein fluorescence in conjunction with visible signs of death (blebbing or swelling). Middle: Intensity profile (blue line) of target cell intracellular calcein showing a clear decrease and decay after the lytic hit. Bottom: Time line defining the phases migration, conjugation, delivery of the lytic hit, and attachment, and the times that were assessed from the experimental data. Time (1) = time to lytic hit, time (2) = time to death, time (3) = conjugation time, and time (4) = attachment time). (B) Time-lapse imaging data showing fluorescence (top), bright-field (middle), and overlay (bottom). An NK cell (red cell body marked by white arrowhead) migrated (Mig, frame 1) to form a conjugate with a target cell (green, star; Conj, frames 2-5), followed by attachment (Att, frame 6) and resumed free migration (Mig, frame 7). At frame 3, the NK cells delivered a lytic hit triggering calcein leakage, which is seen as decreased green fluorescence intensity (frames 3-7) and visible signs of target cell death (frames 4-7). White lines in the overlay images show the NK cell trajectory. Indicated times are hours: minutes. Scale bar indicates 15 μm.
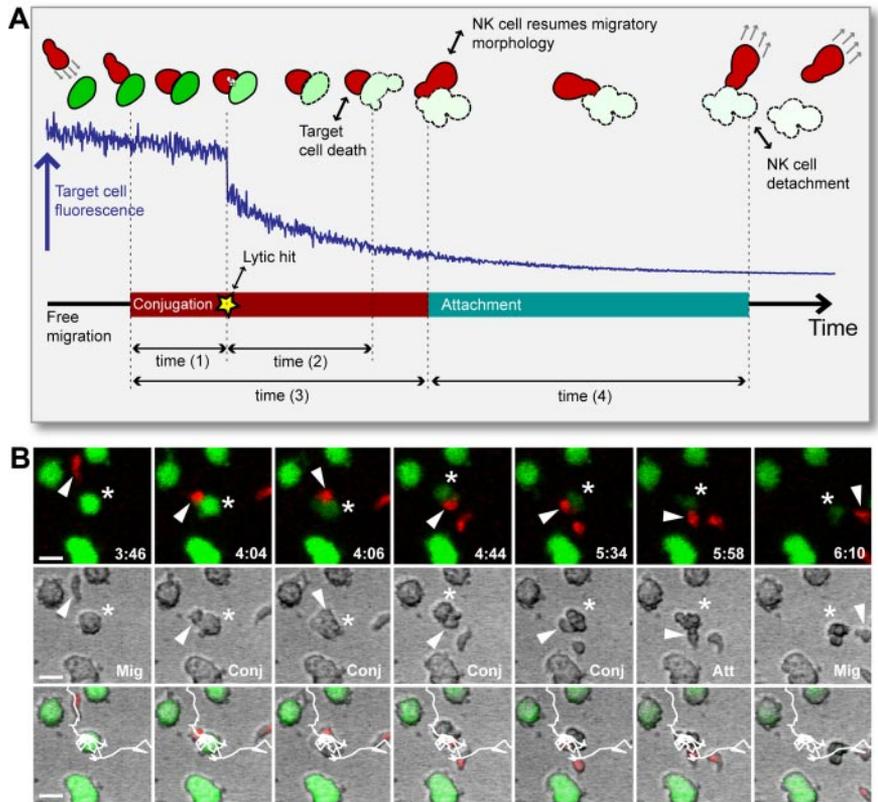
decay of calcein fluorescence intensity. Because analysis of morphology remains one of the most decisive ways to distinguish cell death, target cell death was scored when apoptotic blebbing or membrane explosion was observed. In 93% of the killing events, a distinct fluorescence decrease was observed after NK cell conjugation; no clear decrease was observed in the remaining lytic interactions. Distinct calcein decreases were not observed in the nonlytic NK interactions (supplemental Figure 3), allowing the

time between onset of conjugation and delivery of lytic hit to be quantified for the majority of interactions. The delivery of a lytic hit most often occurred rapidly after conjugation, taking less than 20 minutes in 76% of the killing events (Figure 3C). After the lytic hit, macroscopic signs of death became visible within 20 minutes for 79% of events (Figure 3D). Delivery of a detectable lytic hit was lethal for target cells; visible signs of cell death were observed in 99% of cells receiving a measurable lytic hit. Initiation of death
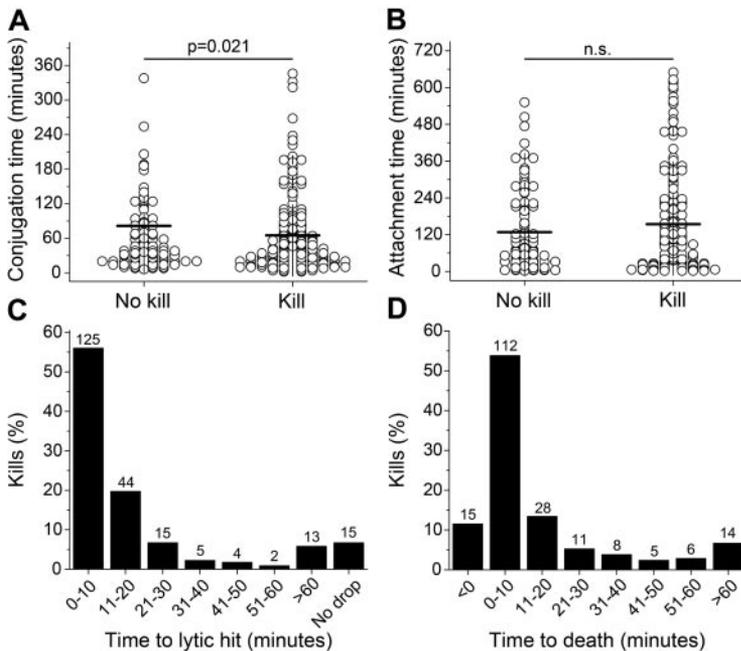

Figure 3. Timing of basic NK cell behavior. (A) Conjugation times for nonlytic and lytic interactions. (B) Attachment times for nonlytic and lytic interactions. (C) Distribution of times to lytic hit. (D) Distribution of times to target cell death.
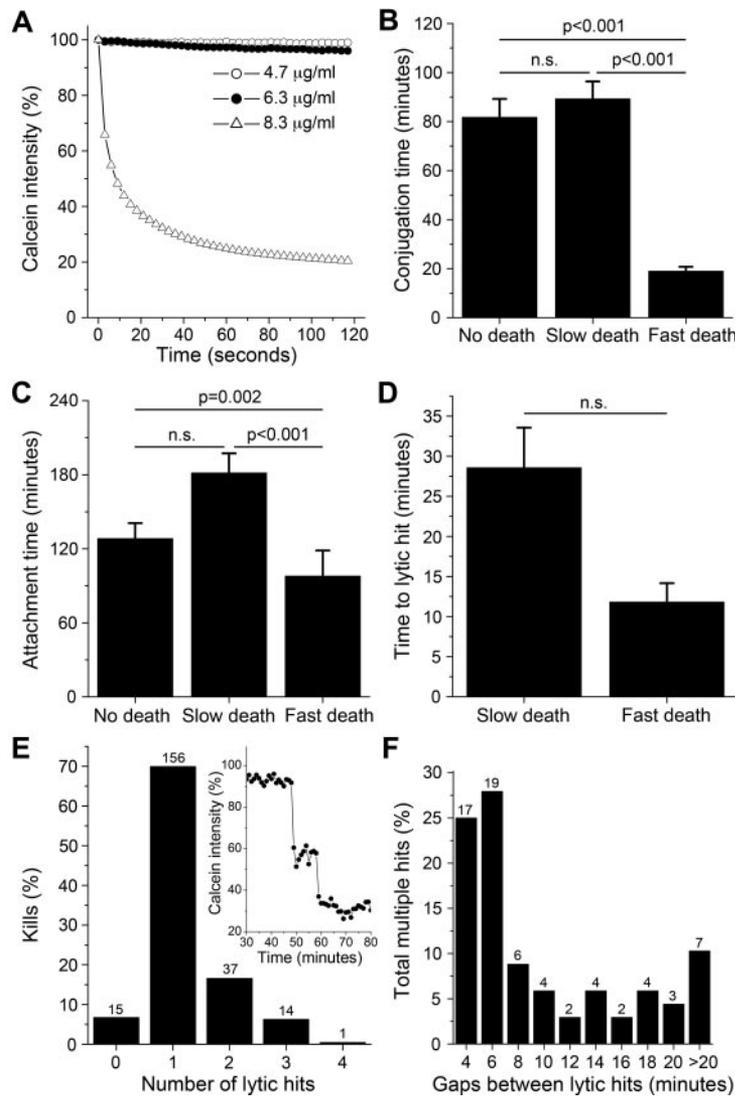
Figure 4. Correlation between speed and strength of the NK response. (A) Calcein intensity profiles for 293T cells treated with melittin. (B-C) Conjugation (B) and attachment (C) times for nonlytic interactions and lytic interactions resulting in slow and fast target cell death. (D) Time to lytic hit for slow or fast target cell death. (E) Percentage of kills over number of lytic hits. Inset: example of a calcein decay showing 2 consecutive hits. (F) Distribution of time gaps between lytic hits. Error bars indicate SE. n.s. indicates $P > .05$. Values above bars in panels E and F indicate n.

occurred within 60 minutes of the lytic hit for the majority (93%) of the lytic events (Figure 3D). In summary, for the majority of events scored, NK cells delivered their lytic hits fast and the subsequent onset of target cell death followed rapidly afterward.

**Correlation between speed and strength of the NK response**

Although a lytic hit was observed in the majority of interactions, the profiles of the corresponding calcein fluorescence decay varied significantly. In general, the decays showed a decrease in intensity corresponding to the lytic hit, followed by a slower phase of decay. To characterize this further, the rate of fluorescence decrease after the lytic hit was approximated by fitting an average lifetime to the decay profile for each individual target cell. Broadly, the rate of target cell death could be separated into 2 main groups: fast (35%) and slow (65%).[25] Supporting the functional reality of these 2 groups, 90% of the fast target cell death events were visually observed as rapid cell swelling and bursting, and 90% of the slow target cell death events were accompanied by cell blebbing consistent with apoptosis (a representative example of each can be found in supplemental Figure 5).

Rapid swelling and bursting of the cell membrane can be induced by high levels of perforin and apoptotic blebbing can be induced using nonlethal concentrations of perforin in combination with granzymes.[26] This suggests that the fast and slow death events observed could be coupled to the amount of perforin released by the NK cell. To test this, calcein-labeled 293T cells were treated with melittin, a pore-forming, cytolytic peptide from bee venom that is structurally similar to perforin.[27-29] Melittin induced cell lysis only at higher concentrations, as detected by a sudden calcein decay and membrane explosion, similar to the fast death observed (Figure 4A and supplemental Video 1).

Strikingly, both mean conjugation (Figure 4B) and attachment (Figure 4C) times were significantly shorter for NK-target interactions leading to fast target cell death. Displacement during attachment for cells dying a slow death (96 μm) was significantly larger than for cells dying fast (57 μm) or not dying (58 μm). Furthermore, the decision to deliver the lytic hit was approximately 3 times faster for kills leading to fast rather than slow death (Figure 4D). Strikingly, the time from lytic hit to end of conjugation was approximately 8 times faster for kills leading to fast (7.2 ± 2.4 minutes) rather than slow (56.6 ± 6.4 minutes) death ($P < .001$). These data clearly show there is a correlation between the speed and strength of the NK cell response.

Figure 5. A minority of NK cells were responsible for a majority of the killing events. (A) Percentage of NK cells forming increasing number of conjugates during the 12-hour assay. (B) Percentage of NK cells responsible for the increasing number of kills. (C) Cumulative percentage of NK cells (black bars, left axis) and cumulative percentage of kills (gray line, right axis) compared with the number of kills performed. (D) Chance of killing (%) at each successive interaction with a target cell for NK cells killing at least one target during the experiment. For panels A, B, and D, the numbers above the bars represent the number of NK cells.
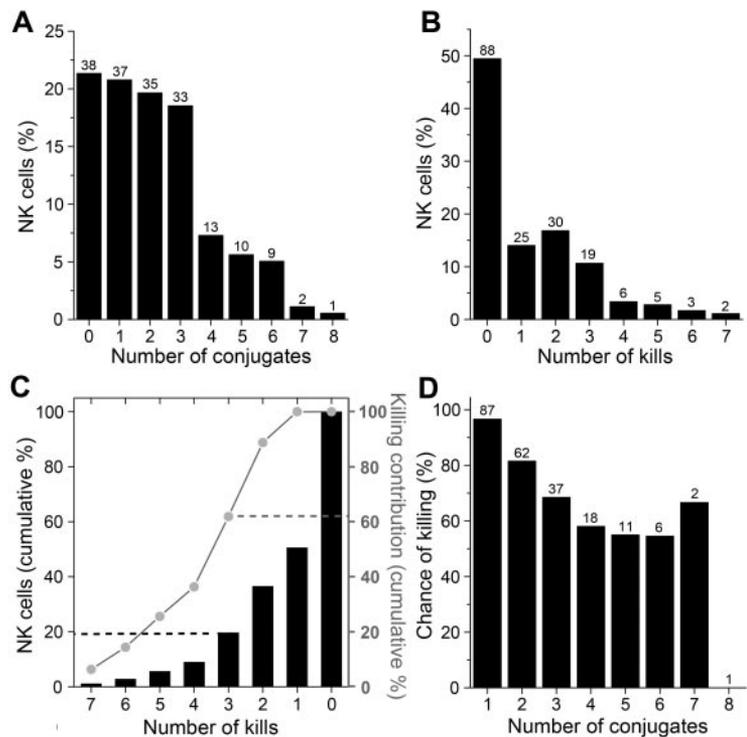
NK cells can deliver multiple lytic hits against a single target cell

Multiple distinct decreases were observed in some of the calcein decay profiles, interpreted as delivery of several lytic hits. Analysis showed that NK cells delivered between 0 and 4 hits during a single target interaction. A single lytic hit was observed in the majority of kills, whereas in 22% of cases, between 2 and 4 lytic hits were observed (Figure 4E). Both conjugation and attachment were slightly longer for multiple compared with single hits (supplemental Figure 4A-B). However, there was no striking difference in the time to lytic hit nor the speed of death for target cells receiving a single or multiple hits when hits in the fast and slow groupings were compared separately (supplemental Figure 4C-D). Successive lytic hits were delivered within short time delays; 53% of hits were delivered within 6 minutes from the previous hit (Figure 4F). In summary, these data suggest that NK cells can deliver separate packages of lytic granules arriving at different times against a single target cell.

A minority of NK cells were responsible for a majority of the killing events

By tracking each NK cell and following its complete conjugation history, it was found that the NK cells formed between 0 and 8 conjugates each within the 12-hour imaging period. A majority (80%) of the NK cells formed 0-3 conjugates and the remaining 20% formed 4-8 conjugates, giving an average of 2.16 conjugates per NK cell (Figure 5A). In total, 223 killing events were scored, yielding a population average of 1.25 kills per NK cell. Strikingly, 49% (n = 88) of NK cells did not kill at all, whereas some cells killed as many as 7 target cells (Figure 5B). NK cells killing 3 or more target cells comprised 20% of the total NK cell population but were responsible for 62% of the killing (Figure 5C). Analysis of the lytic NK cells showed that the chance of killing decreased with increasing numbers of target cell encounters (Figure 5D), possibly

because of depletion of cytotoxic molecules. Clearly, a small percentage of the NK cells were responsible for the majority of killing events and the probability of killing decreased with increasing numbers of target cell encounters.

NK cells can be categorized into 5 classes based on their contact/killing history

Broadly, individual NK cells could be divided into groups based on their contact and killing behavior (Figure 6A). Plotting the complete contact/killing histories for individual NK cells (Figure 6B) revealed that NK cells that were engaged in both lytic and nonlytic interactions could be further subdivided into NK cells that killed until they appeared to be unable to kill, thus being "exhausted," and NK cells that behaved more stochastically, alternating between killing and nonkilling in an apparently random fashion. Therefore, there were 5 distinct NK cell classes: (1) NK cells that did not interact with target cells (n = 38), (2) NK cells that did not kill (n = 50), (3) NK cells that killed all target cells encountered (n = 54), (4) exhausted NK cells (n = 30), and (5) NK cells that killed stochastically (n = 6). Overall, 178 NK cells were distributed among 32 distinct contact/killing behaviors with 1-12 behaviors in each class (Figure 6B). These classes contained 3%-30% of the NK cells (Figure 6C). A fraction of the NK cells (12.9%) were observed to die during the assay, with approximately half of those coming from the pool of cells that never interacted with target cells (see supplemental Figure 6 for a detailed analysis of NK cell death). In summary, most NK cells showed a consistent behavior, being inactive, lytic, or nonlytic. If an NK cell was active, it would generally remain so until it stopped killing.

These striking differences observed between individual cells combined with their consistency in killing behavior indicated a significant heterogeneity of the NK population. To test this, we ran computer simulations assuming all NK cells behaved as the
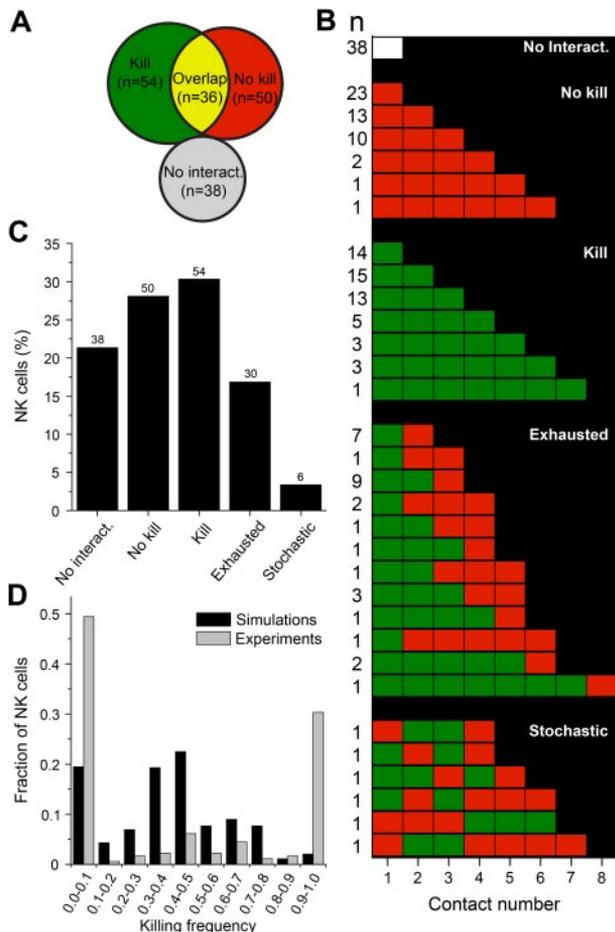
Figure 6. NK cells can be classified based on their contact/killing history. (A) Venn diagram depicting the distribution of NK cells based on whether they always killed (green), never killed (red), sometimes killed (yellow overlap), or never encountered target cells (white). (B) Contact history of individual NK cells arranged into 5 different classes. The columns represent the number of conjugates formed and each row represents a conjugation/killing sequence. White represents no interaction; red, nonlytic interaction; and green, lytic interaction. Numbers on the left indicate the number of NK cells observed. (C) Frequency of each group as a percentage of the total NK population. (D) Fraction of NK cells that exhibited the indicated killing frequency in the experiments (gray bars) and simulations (black bars). The killing frequency is the fraction of interactions that resulted in target cell death out of all of the interactions in which the NK cell participated. NK cells that never encountered target cells in the experiments or simulation were given a killing frequency of zero and were included in the analysis (thus contributing to the bars at 0.0-0.1).

"average" NK cell. The likelihood of killing was assumed to be 58% in all NK-target encounters and the conjugation times and gaps between conjugations were assumed to be distributed as in the experimental data. The populations of NK cells killing 0%-10% or 90%-100% were much larger in the experimental compared with the simulated data, indicating that the observed distribution of killing frequencies was unlikely to occur by chance (Figure 6D). This confirmed that the observed heterogeneity was real and was not a consequence of random events.

Serial killers are larger and show a faster and stronger response than other NK cells

Ten NK cells (5.6% of the total population) were particularly cytolytic, with 5 or more kills. These serial killers were responsible for 26% of the total number of kills. Plotting the distributions of when conjugation periods and lytic events occurred for the individual serial killers (Figure 7A) showed that the majority of the

killing events occurred early in the assay even if a few killings were also detected at later times and then seemed to be coupled to longer conjugation times (eg, cell numbers 4, 7, and 10). For some NK cells (eg, cell numbers 2, 8, and 9), successive kills occurred in short time intervals, whereas for others (eg, 4 and 5), time intervals were longer. The behavior of serial killers was compared with that of all other cytolytic NK cells. As opposed to the other NK cells, serial killers induced rapid, necrotic target cell death in the majority of killing events (Figure 7B). The conjugation length and time to lytic hit was approximately 2 times shorter for serial killers than other killers, whereas the time to death was approximately 4 times shorter (Figure 7C-E), indicating that serial killers launch significantly faster and stronger lytic responses than average. Intriguingly, serial killers were also larger than nonserial killers (Figure 7F).

Discussion

The law of the vital few, or the Pareto principle, states that the majority of effects come from a minority of causes. The data presented herein show that this is true also for polyclonal NK cell–mediated killing of 293T tumor cells, in which a minority of NK cells was responsible for the majority of target cell lysis. One reason that this has not been thoroughly described previously is that cell-mediated cytotoxicity assays are often based on population averages and lack detailed information about individual cell behavior over time. Our observations were made possible through use of a microchip-based, live-cell migration and killing assay with single-cell resolution.[21]

The present study allowed a detailed characterization of single NK cell behavior over time by recording the entire contact history of NK cells. This allowed classification of the NK cells based on their cytotoxic response. NK cells revealed remarkable binary commitment toward either killing or not killing, and killing would occur until NK cell exhaustion that was likely due in part to depletion of cytolytic granules.[17] In a small minority of cells (6 of 178, 3%) a clear dedication was lacking, with cells stochastically alternating between killing and nonkilling. Interestingly, the speed of target cell death varied significantly and could be coupled to apoptotic blebbing (slow, 65% of killing events) and necrosis (fast, 35% of killing events). Apoptosis is a clean death, resulting in phagocytosis and subsequent antigen presentation, whereas necrosis results in uncontrolled release of cellular content coupled to immune activation and inflammation. The speed of target cell death was correlated with the quantity of pore-forming molecules delivered by the NK cell. Interestingly, serial killers were particularly efficient, representing approximately 6% of cells contributing 26% of lytic events. Underlying this efficiency, they responded stronger and faster than other NK cells. Resolving the mechanisms behind this link between speed and strength in the response is a challenge for future work, but it is possible that "hesitation" in progressing through checkpoints required for killing could slow down the process and at the same time decrease the strength of the response. Alternatively, rapid clearance of checkpoints could be coupled to high amounts of mobilized granules. Although serial killers were larger, the coupling behind size and serial killing remains unknown. IL-2–activated NK cells grow in size, which could reflect particularly efficient cytokine-mediated activation. It will be important to investigate these observations in both naive and IL-15–cultured NK cells. In summary, our data are consistent
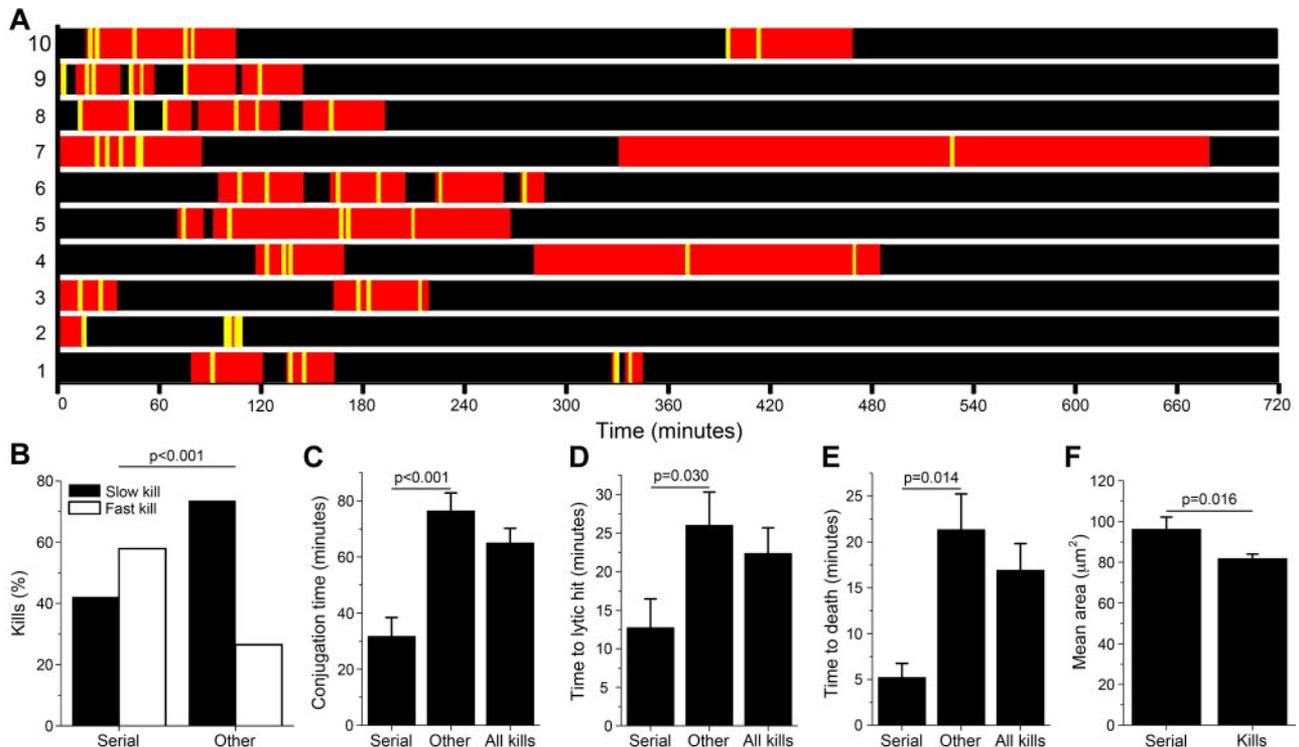
Figure 7. Serial killers are larger and show stronger and faster responses. (A) Scheme showing conjugation periods (red) and target cell killing events (yellow lines) for the 10 detected NK serial killers. (B) Percentage of fast and slow kills and times (C-E) measured for serial killers (serial), all cytolytic interactions (all kills), and all cytolytic interactions except those performed by serial killers (other). (C) Conjugation time. (D) Time to lytic hit. (E) Time to target cell death. (F) Mean cell area for serial killers (serial) and all NK cells that killed at least one target cell during the experiment (kills).

with a model in which a small fraction of cells drive both tumor elimination and inflammation.

The correlation between the frequency of CD107a$^+$ (ie, degranulating) cells (approximately 15%) and lytic NK cells measured at the single-cell level (51% or 34% when looking only at the first 4 hours of the assay) was poor. Even though the experimental conditions were not identical in these assays, this discrepancy indicates that FACS-based CD107a measurements could underestimate the frequency of responding NK cells. Although NK cell cytotoxicity was directly observable, our experimental setup did not allow measurement of cytokine secretion and, therefore, it was not possible to correlate this to certain types of behavior such as killing or nonkilling. However, a recent study demonstrated that there was no difference in the levels of MIP-1β and IFN-γ production at the single-cell level between lytic and nonlytic interactions,[30] suggesting that no differences in the levels of cytokine secretion would have been observed between lytic and nonlytic NK cells.

Phenotypic information regarding NK receptor expression is lacking in the present study and therefore cannot be correlated with the definition of subsets or any specific observation (eg, speed of lytic hit or fast or slow death). An attempt to phenotypically identify serial killers by 12-color FACS based on the assumption that they would display a preferential loss of perforin was unsuccessful because no such clear population was observed. Similarly, looking at perforin loss in specific subsets revealed inconclusive results and could be a consequence of the subsets tested. Gating of NK cells low in perforin after coincubation did not identify serial killers and, therefore, perforin loss might not be correlated directly with the amount of target cells killed. This unsuccessful attempt is probably due in part to the inability to obtain single-cell data over time by flow cytometry. Identification

of serial killers could be addressed, for example, by FACS sorting of specific subsets or use of phenotyped NK cell clones. However, technical challenges remain, such as accurate selection of NK subsets and high-throughput, yet detailed, analysis of time-lapse imaging data. Therefore, the origins of the observed heterogeneity remain to be explored in future studies. Nonetheless, computer simulations confirmed that the observed heterogeneity was real and this is the first study to analyze the entire contact history of a population of NK cells.

The importance of processes regulating NK-target cell contact time is recognized, but the responsible mechanisms are still not well characterized.[31] Similar to cytotoxicity, the formation of a stable conjugate depends on a balance between activating and inhibitory signals received by NK cells. Activating signals result in symmetrical spreading and conjugation, whereas inhibitory signaling breaks NK spreading, encouraging NK cell migration.[32] Considering those results, it is somewhat unexpected that the mean conjugation times measured herein were shorter for lytic than nonlytic interactions. It is possible that our data are skewed by the relatively infrequent sampling and the definition of a conjugate (minimum conjugate length, 4 minutes), because large proportions of NK cells have been observed to form dynamic, short-lasting contacts with target cells.[33] However, we clearly observed a fraction of nonlytic interactions with relatively long conjugation times. It is possible that the thresholds for cytotoxicity and conjugation are differently regulated, so that in our system, several of the nonlytic interactions received sufficient activating signals to maintain conjugation but not enough to trigger degranulation. NK cells that delivered a strong cytotoxic response leading to fast target cell death were observed to terminate the conjugation phase much more rapidly than NK cells inducing slow target cell death. This indicates that the NK cell commitment to conjugation is

dependent on the viability and membrane integrity of the target cell. Furthermore, target cells often remained attached to NK cells after conjugate break-up. It is likely that 2 separate mechanisms regulate NK-target cell contact times, one that terminates conjugation (possibly by weakening the intercellular bonds) and a second that requires generation of mechanical forces driving the 2 cells apart (largely driven by NK cell motility).

In conclusion, in the present study, we have quantified NK cell heterogeneity in the cytotoxic response, enabling grouping of NK cells into 5 distinct classes. This was made possible through an experimental approach in which individual NK and target cells could be followed over extended times. Future challenges include determining how NK cell classes are correlated with phenotype, the cell biologic mechanisms behind multiple hits, and the link between speed and strength of the response.

Acknowledgments

Authorship

Contribution: B.V. designed and performed the research, analyzed the data, and wrote the manuscript; P.E.O., M.A.K., S.P., and K.G. analyzed the data; E.F. and M.E. performed the research and analyzed the data; M.S.-S. designed and performed the computer simulations; K.-J.M. designed the research; R.M. designed the research and critically read the manuscript; and B.Ö. conceived the study, designed the research, and wrote the manuscript.

Conflict-of-interest disclosure: The authors declare no competing financial interests.

Correspondence: Björn Önfelt, Department of Applied Physics, Albanova University Center, KTH Royal Institute of Technology, SE-10691, Stockholm, Sweden; e-mail: bjorn.onfelt@ki.se.

References

1. Kiessling R, Klein E, Wigzell H. "Natural" killer cells in the mouse. I. Cytotoxic cells with specificity for mouse Moloney leukemia cells. Specificity and distribution according to genotype. *Eur J Immunol.* 1975;5(2):112-117.

2. Yokoyama WM, Kim S, French AR. The dynamic life of natural killer cells. *Annu Rev Immunol.* 2004;22:405-429.

3. Orange JS. Formation and function of the lytic NK-cell immunological synapse. *Nat Rev Immunol.* 2008;8(9):713-725.

4. Lanier LL. NK cell recognition. *Annu Rev Immunol.* 2005;23:225-274.

5. Davis DM, Chiu I, Fassett M, Cohen GB, Mandelboim O, Strominger JL. The human natural killer cell immune synapse. *Proc Natl Acad Sci U S A.* 1999;96(26):15062-15067.

6. Krzewski K, Strominger JL. The killer's kiss: the many functions of NK cell immunological synapses. *Curr Opin Cell Biol.* 2008;20(5):597-605.

7. Eissmann P, Davis DM. Inhibitory and regulatory immune synapses. *Curr Top Microbiol Immunol.* 2010;340:63-79.

8. Wulfing C, Purtic B, Klem J, Schatzle JD. Stepwise cytoskeletal polarization as a series of checkpoints in innate but not adaptive cytolytic killing. *Proc Natl Acad Sci U S A.* 2003;100(13):7767-7772.

9. Orange JS, Harris KE, Andzelm MM, Valter MM, Geha RS, Strominger JL. The mature activating natural killer cell immunologic synapse is formed in distinct stages. *Proc Natl Acad Sci U S A.* 2003;100(24):14151-14156.

10. Brown AC, Oddos S, Dobbie IM, et al. Remodelling of cortical actin where lytic granules dock at natural killer cell immune synapses revealed by super-resolution microscopy. *PLoS Biol.* 2011;9(9):e1001152.

11. Griffiths GM, Tsun A, Stinchcombe JC. The immunological synapse: a focal point for endocytosis and exocytosis. *J Cell Biol.* 2010;189(3):399-406.

12. Kagi D, Ledermann B, Burki K, et al. Cytotoxicity mediated by T cells and natural killer cells is greatly impaired in perforin-deficient mice. *Nature.* 1994;369(6475):31-37.

13. Waterhouse NJ, Sutton VR, Sedelies KA, et al. Cytotoxic T lymphocyte-induced killing in the absence of granzymes A and B is unique and distinct from both apoptosis and perforin-dependent lysis. *J Cell Biol.* 2006;173(1):133-144.

14. Eriksson M, Leitz G, Fallman E, et al. Inhibitory receptors alter natural killer cell interactions with target cells yet allow simultaneous killing of susceptible targets. *J Exp Med.* 1999;190(7):1005-1012.

15. Garrod KR, Wei SH, Parker I, Cahalan MD. Natural killer cells actively patrol peripheral lymph nodes forming stable conjugates to eliminate MHC-mismatched targets. *Proc Natl Acad Sci U S A.* 2007;104(29):12081-12086.

16. Martz E. Multiple target cell killing by the cytolytic T lymphocyte and the mechanism of cytotoxicity. *Transplantation.* 1976;21(1):5-11.

17. Bhat R, Watzl C. Serial Killing of Tumor Cells by Human Natural Killer Cells – Enhancement by Therapeutic Antibodies. *PLoS One.* 2007;2(3):e326.

18. Lopez JA, Brennan AJ, Whisstock JC, Voskoboinik I, Trapani JA. Protecting a serial killer: pathways for perforin trafficking and self-defence ensure sequential target cell death. *Trends Immunol.* 2012;33(8):406-412.

19. Liu D, Martina JA, Wu XS, Hammer JA, 3rd Long EO. Two modes of lytic granule fusion during degranulation by natural killer cells. *Immunol Cell Biol.* 2011;89(6):728-738.

20. Li P, Zheng G, Yang Y, et al. Granzyme B is recovered by natural killer cells via clathrin-dependent endocytosis. *Cell Mol Life Sci.* 2010;67(18):3197-3208.

21. Khorshidi MA, Vanherberghen B, Kowalewski JM, et al. Analysis of transient migration behavior of natural killer cells imaged in situ and in vitro. *Integr Biol (Camb).* 2011;3(7):770-778.

22. Frisk TW, Khorshidi MA, Guldevall K, Vanherberghen B, Onfelt B. A silicon-glass microwell platform for high-resolution imaging and high-content screening with single cell resolution. *Biomed Microdevices.* 2011;13(4):683-693.

23. Alter G, Malenfant JM, Altfeld M. CD107a as a functional marker for the identification of natural killer cell activity. *J Immunol Methods.* 2004;294(1-2):15-22.

24. Onfelt B, Nedvetzki S, Yanagi K, Davis DM. Cutting edge: Membrane nanotubes connect immune cells. *J Immunol.* 2004;173(3):1511-1513.

25. Guldevall K, Vanherberghen B, Frisk T, et al. Imaging immune surveillance of individual natural killer cells confined in microwell arrays. *PLoS One.* 2010;5(11):e15453.

26. Keefe D, Shi L, Feske S, et al. Perforin triggers a plasma membrane-repair response that facilitates CTL induction of apoptosis. *Immunity.* 2005;23(3):249-262.

27. Duke RC, Witter RZ, Nash PB, Young JD, Ojcius DM. Cytolysis mediated by ionophores and pore-forming agents: role of intracellular calcium in apoptosis. *FASEB J.* 1994;8(2):237-246.

28. Laine RO, Morgan BP, Esser AF. Comparison between complement and melittin hemolysis: anti-melittin antibodies inhibit complement lysis. *Biochemistry.* 1988;27(14):5308-5314.

29. Persechini PM, Ojcius DM, Adeodato SC, Notaroberto PC, Daniel CB, Young JDE. Channel-forming activity of the perforin N-terminus and a putative alpha-helical region homologous with complement C9. *Biochemistry.* 1992;31(21):5017-5021.

30. Yamanaka YJ, Berger CT, Sips M, Cheney PC, Alter G, Love JC. Single-cell analysis of the dynamics and functional outcomes of interactions between human natural killer cells and target cells. *Integr Biol (Camb).* 2012;4(10):1175-1184.

31. Davis DM. Mechanisms and functions for the duration of intercellular contacts made by lymphocytes. *Nat Rev Immunol.* 2009;9(8):543-555.

32. Culley FJ, Johnson M, Evans JH, et al. Natural killer cell signal integration balances synapse symmetry and migration. *PLoS Biol.* 2009;7(7):e1000159.

33. Deguine J, Breart B, Lemaitre F, Di Santo JP, Bousso P. Intravital imaging reveals distinct dynamics for natural killer and CD8(+) T cells during tumor regression. *Immunity.* 2010;33(4):632-644.